Fermi surfaces and phase shifts of PdIn and other β brasses

A. E. Dunsworth*
Division of Physics, National Research Council of Canada, Ottawa, Ontario, Canada
(Received 12 May 1975)

The de Haas–van Alphen frequency branches of PdIn are explained with a Fermi surface similar to those of CuZn and AgZn. Some new measurements provide better information in the region near ⟨100⟩. The Fermi-surface areas of PdIn and AgZn are fitted with adjustable phase shifts in an augmented-plane-wave formalism. The phase shifts of PdIn are also fitted while varying the energy parameter. The phase shifts and Friedel sums behave as expected when the methods used previously for monatomic metals are generalized to diatomic ordered alloys. The results suggest that ~ 1 electron is shifted from the In to the Pd atom.

I. INTRODUCTION

The three β brasses CuZn, AgZn, and PdIn have been studied experimentally for many years but only recently has the correct identification of theoretical and observed de Haas–Van Alphen (dHvA) branches been made. Data taken by pulsed-field methods were presented by Jan, Pearson, and Saito[1] for all three alloys and by Karlsson[2] for PdIn and CuZn. The amount of data was much increased when the field-modulation technique was used to remeasure first PdIn and CuZn,[3] and then AgZn.[4] The similarity between the areas of the three alloys when expressed in units of $(2\pi/a)^2$ was noted immediately.[1] The free-electron model suggested a closed first-band section which should be observed in all angular positions. Various orbits were identified with this piece, leading to partial explanations of other branches. Unfortunately, the orbit actually arising from the first band was seen only over a very restricted range in CuZn and in broken sections in PdIn. The more complete recent data in[3] PdIn and[4] AgZn allowed inversion of the frequency branch and the expected first-band shape was found. There is still no explanation for the absence of the first-band signals over large regions in CuZn. The band structure of Skriver[5,6] on CuZn agreed quite well with experiment and made the orbit identifications obvious. A similar calculation[7] of AgZn agreed in the same way. This paper presents some new measurements on PdIn taken to clarify its Fermi surface in light of the two previous band structures and shows how the PdIn Fermi surface can be explained. Furthermore, a phase-shift parametrization is used to fit the Fermi surfaces of PdIn and AgZn. By fitting certain radii of the PdIn surface, it is shown that the phase shifts and Friedel sums as a function of energy behave in a similar way to those found in monatomic metals by other workers, thereby extending to ordered alloys this useful technique of dHvA data reduction.

II. β BRASSES

The β brasses form in a CsCl structure with two atoms per cell. If one atom is taken at (0, 0, 0) then the other is at $(\frac{1}{2}, \frac{1}{2}, \frac{1}{2})$ in the primitive cubic cell. For both atoms identical, this arrangement is body-centered cubic. The three alloys discussed in the paper all have three electrons per cell (in PdIn, In contributes all three electrons and in AgZn and CuZn, Zn contributes two electrons) and a Brillouin zone and Fermi surface similar to that shown in Fig. 1. The prominent orbits will be discussed briefly here to avoid confusion in the later sections. The second-band electrons form the large speckled surface in Fig. 1 where the front section has been removed for clarity. The orbits called the arm, square hole, neck, muffin, and triangular hole all arise from this surface while another orbit arises from the closed first-band octahedron at R.

The triangular hole orbit is the prominent experimental feature common to all the alloys. Its large range of existence caused it to be mistaken for the octahedron at one time. The octahedron is seen strongly in AgZn, less so in PdIn and only in certain regions in CuZn. The remaining orbits are seen only near symmetry axes. Table I shows a summary of the observed major frequency branches in the three alloys along with the regions of Fermi surface responsible for them. The data branch labels correspond to those given in earlier papers.

Since the Fermi surfaces of these β brasses have the free-electron topology, it is natural to expect a phase-shift parametrization scheme to describe the data fairly easily with parameters near zero. Two variants were used for fitting as mentioned below, with details left for Sec. III. The first method fits some observed areas in high-symmetry directions with a relatively low-order augmented-plane-wave (APW) matrix. The aim is to find a numerical description of the Fermi surface in terms of five or six phase shifts at the free-elec-

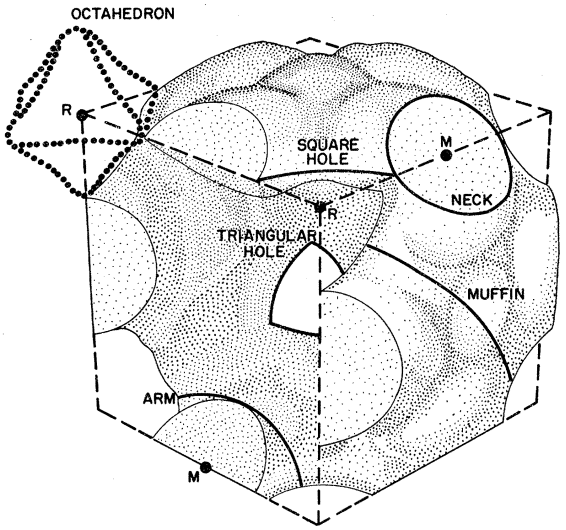

FIG. 1. Brillouin zone and Fermi surface of a β brass with three electrons per cell. The front surface is cut away to show interior orbits.

tron energy. The agreement is discussed under the heading of each alloy. The second fits phase shifts in a symmetrized APW formalism to radii deduced from the areas of PdIn. This fit is used to explore the energy dependence of the phase shifts and Friedel sums in a more fundamental way than simple data description.

A. PdIn

The main body of data for PdIn are given by Jan and Perrott,[3] part of which is shown in Fig. 2. The new measurements shown in Fig. 3 were made with the same sample and method used previously.[3] The (100) data show a clear separation of F_5 and F_3 with a slight gap between them. There is no indication of F_3–F_5 overlap as found before. In the (210) plane the separation is less clearcut with F_3 and F_{11} becoming mixed and several side branches appearing. These side branches also occur in the (110) plane and near the ⟨710⟩ in the (710) plane. They have the common features of lying ~ 5°–15° from ⟨100⟩, falling between F_3 and F_5 and existing only over a small angular range. Since the ⟨710⟩ is only 8° from ⟨100⟩, this plane fits in with the trend.

These orbits are caused by magnetic breakdown[8] between the octahedron and the square hole. In the nonrelativistic case, the bands touch along the *RM* line. The spin-orbit effects generate a small gap which causes partial breakdown. Frequencies corresponding to three breakdown areas have been observed near the ⟨100⟩ axis. The orbit F_3 is formed by electrons spending half an orbit on the octahedron and half on the square hole. This orbit is prominent in the medium breakdown region and is the only orbit expected if there is a complete breakdown. Old data were reexamined with care being given to the significance of small Fourier amplitudes. The existence of branch F_6 lying slightly below F_1 is doubtful and the upper branch of F_1 at ⟨110⟩ in the (110) plane has a range of $\leq 1°$.

The inversion of the F_5 and F_2 branches to give an octahedron[3] along with the band structures of Skriver[5–7] allow interpretation of all branches in PdIn. F_1 comes from the second-band noncentral

TABLE I. The branch labels of experimental data in PdIn, AgZn, and CuZn and their origin on the Fermi surface.

Origin	PdIn	AgZn	CuZn
octahedron	F_5, F_2	F_5	F_5, F_3
triangular hole	F_1	F_1	F_1
neck	F_9	F_9	F_2
muffin	F_4	F_4	...
square hole	F_{11}	...	...
arm	F_1'	...	...
noncentral orbits[a]	...	...	F_4, unlabeled points near F_2[b]
breakdown orbit[c]	F_3	...	F_3
?	...	F_7	F_{10}

[a]References 5 and 6.
[b]Reference 3.
[c]$\frac{1}{2}$(octahedron + square hole).

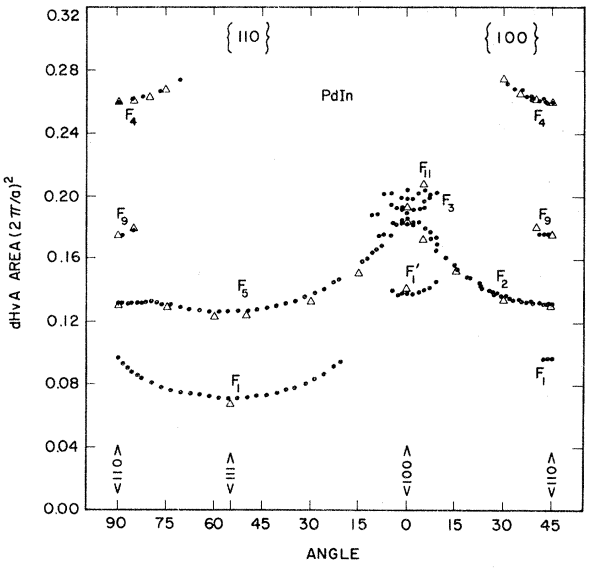

FIG. 2. Dots are the observed data of PdIn in the (110) and (100) planes. The Δ's are calculated values for the *s*, *p*, *d* phase shifts −0.252, 0.003, −0.138 of Pd and 0.048, 0.279, 0.000 of In at the free-electron energy.

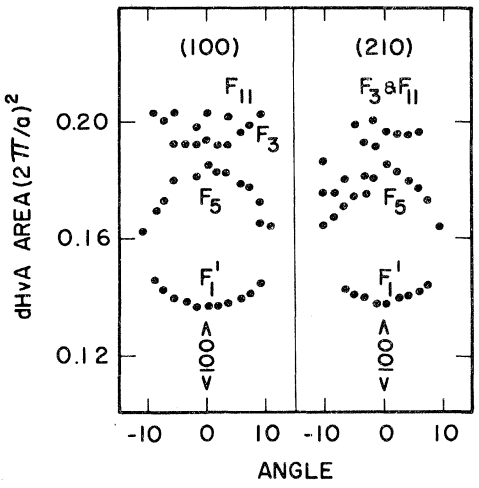

FIG. 3. Detail of the frequency branches around ⟨100⟩ in the (100) and (210) planes.

triangular hole along ⟨111⟩, F_2 and F_5 from the first-band octahedron at R, F_4 from the second-band muffin centered at X, F_9 from the second-band necks at M, F_{11} from the second-band square hole at R and F_1' from the noncentral arm parallel to ⟨100⟩.

Some areas calculated from a phase-shift parametrization are shown in Fig. 2 for a range of angles. All the calculated orbits are central except for F_1 and F_1' which were found by searching parallel slices of Fermi surface perpendicular to the orbit direction for an extremum. The agreement is quite good overall. In this fit, the octahedron square-hole splitting at ⟨100⟩ is forced to be correct at the expense of a low value for the triangular hole at ⟨111⟩.

The band structure has been calculated by Cho[9] who obtained a topologically correct Fermi surface with nearly the right dimensions. His comparison of theoretical and observed areas was made difficult by the lack of data at that time and problems of correctly relating observed and predicted branches.

The radii used as parameters for fitting are listed in Table II. The three values in the first band were found by inverting the octahedron areas to radii. The errors are estimated from the relative sensitivity of each radius to changes in the number of inversion coefficients. Since the second band cannot be inverted, the radii were deduced from some observed areas in high-symmetry direction. To do this, it is necessary to know the shape of the Fermi-surface piece involved. There is no direct measurement of this so it was assumed that the actual and calculated shapes were the same when the numerically integrated theoretical areas equalled the measured areas. This shape was used to get a simple analytic form relating the area to the radii, for instance πab. The three areas chosen, the neck, square hole, and muffin, all have simple shapes as suggested in Fig. 1. The $M\Gamma$ neck radius (Γ is the zone center) is determined by the neck area and the radius along MR. The MR radius is fixed by the ⟨100⟩ octahedron radius since the sum of these two is one half the cube edge in the absence of spin-orbit splitting. The actual splitting here must be small otherwise the large neck area could not be accounted for. The difference between the ⟨100⟩ square hole and octahedron areas gives the second-band radius along RX (X is the zone face center) since the RM radius is shared by both orbits without spin-orbit effects. The RX radius immediately gives the XR radius of the muffin orbit since the sum of the two is the whole XR distance. The thickness of the muffin $X\Gamma$ follows from this. Therefore, there are three independent radii $M\Gamma$, RX, and $X\Gamma$ in the second band. The errors listed in Table II for the second band are minimum estimates based on the assumptions made above.

B. AgZn

The data for AgZn are given in Dunsworth and Jan[4] and are compared there with the APW band-structure calculations of Skriver.[7] The general features of the Fermi surface are the same as those of PdIn but the data are not so plentiful so several orbits expected are not observed. However, the main features of octahedron and triangular hole are present and have very similar proportions. The data shown in Fig. 4 are compared with areas calculated from the phase-shift parametrization and by Skriver from first principles. The phase-shift agreement is excellent. Some radii deduced from the data are listed in Table II. Since there are insufficient values to form a proper least-squares sum, no fitting of the type described later was done for AgZn.

C. CuZn

The data for CuZn are given by Jan and Perrott[3] and are compared with an APW calculation by Skriver.[5,6] The Fermi surface is very similar to the two previous materials and also shows ex-

TABLE II. Radii from the Fermi surface of PdIn and AgZn in units of $2\pi/a$.

Band	Direction	PdIn	AgZn
1	$R \rightarrow \Lambda$	0.174 ± 0.001	0.174 ± 0.002
1	$R \rightarrow T$	0.267 ± 0.002	0.268 ± 0.002
1	$R \rightarrow S$	0.222 ± 0.001	0.213 ± 0.001
2	$M \rightarrow \Sigma$	0.242 ± 0.002	0.242 ± 0.002
2	$X \rightarrow \Delta$	0.192 ± 0.001	...
2	$R \rightarrow S$	0.229 ± 0.003	...

perimentally some interesting noncentral sections predicted by theory but not observed in either PdIn or AgZn.

The orbit F_3 in CuZn, previously considered to be the square hole, is the breakdown orbit formed from half the octahedron and half the square hole. It is prominent experimentally while the octahedron points below are only weakly observed, suggesting that in CuZn the magnetic breakdown is nearly complete. Indeed a relativistic band structure of Skriver[10] shows the spin-orbit splitting to be very small. This explains the discrepancy of curvature noticed between the calculated bands and the experiments.

Unfortunately, for unknown reasons, the octahedron branch is not observed over large regions of the (110) and (211) planes so no inversion can be done to verify the shape and calculate its radii. For instance, in the (110) plane, the branch is not seen for a range of 70°. It seems unlikely that a spin splitting zero could occur over this wide range. The possibility of magnetic breakdown was checked by Jan[11] who measured the field dependence of the amplitude 10° from the ⟨110⟩ axis, just before the region where the branch vanishes. He finds no unusual amplitude variation. No phase-shift fits have been made for CuZn because the lack of an octahedron inversion removed the basic starting point of the method.

III. APW

The symmetrized-APW (SAPW) method as described by Mattheiss, Wood, and Switendick[12] was followed in constructing the main APW foundation of the calculation. The potential was parametrized by phase shifts ϵ_l and passed into the SAPW matrix elements as logarithmic derivatives $L_l(R,E)$ found from the following equation:

$$L_l(R,E)=(E)^{1/2}\frac{j_l'[(E)^{1/2}R]-n_l'[(E)^{1/2}R]\tan\epsilon_l}{j_l[(E)^{1/2}R]-n_l[(E)^{1/2}R]\tan\epsilon_l},$$

where E is the energy above the APW zero; R is the muffin-tin radius; and j,n,j',n' are the spherical Bessel and Neumann functions and their derivatives. Six phase shifts (s,p, and d from each atom) were available as parameters but, in practice, the d phase shift on the nontransition or noble metal was not varied and was set to zero along with all other phase shifts having $l>2$. Equal muffin-tin radii were taken for each atom; the l sum was cut off at $l=8$ and sufficient SAPW prototype reciprocal-lattice vectors (RLVs) were taken to make the results equivalent to using ~60 unsymmetrized RLVs. No spin-orbit or other corrections were included in the potential. Fermi-surface radii were found by searching for determinant zeros as a function of wave-vector magnitude keeping the search direction and the energy E constant. Using SAPWs removed the problem of closely spaced and double roots found in the unsymmetrized case along the RX and RM lines. Radii chosen along high-symmetry directions ($R\Gamma$, RM, RX, $X\Gamma$, and $M\Gamma$) were used to specify the experimental Fermi surface. The method of deducing these radii from the experimental areas was described in Sec. II A. Radii are chosen rather than areas to reduce computation time since a calculation of an area requires at least five radii, each one of which is in general in a low-symmetry direction thereby further enlarging the number of RLVs needed for given accuracy. A nonlinear minimization scheme[13] designed for functions having the form $\sum_i f_i^2$ was used to determine the best set of phase shifts at each energy.

Examples of the agreement between observed and calculated areas at various places are shown in Fig. 2 and 4. These areas were found using ~25 RLVs in the determinant for the parameters listed in the figures and with E set to the free-electron value. The phase shifts listed are not identically the same as those found using the SAPW scheme but are quite close. The agreement is quite good especially for AgZn.

IV. DISCUSSION

Figure 5 shows the fitting error, phase shifts, and Friedel sums of PdIn as a function of energy

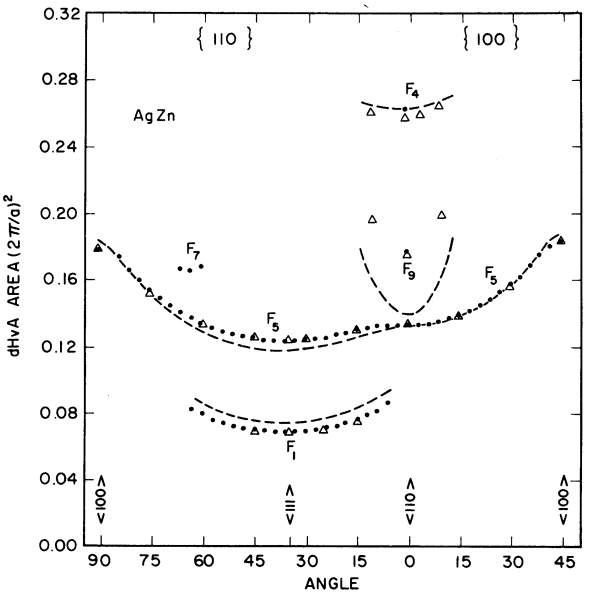

FIG. 4. Dots are the observed data of AgZn in the (110) and (100) planes. The Δ's are calculated values for the phase shifts −0.194, −0.004, −0.142 of Ag and −0.028, 0.289, 0.001 of Zn at the free-electron energy. The broken lines are the results of Ref. 7 from first principles.

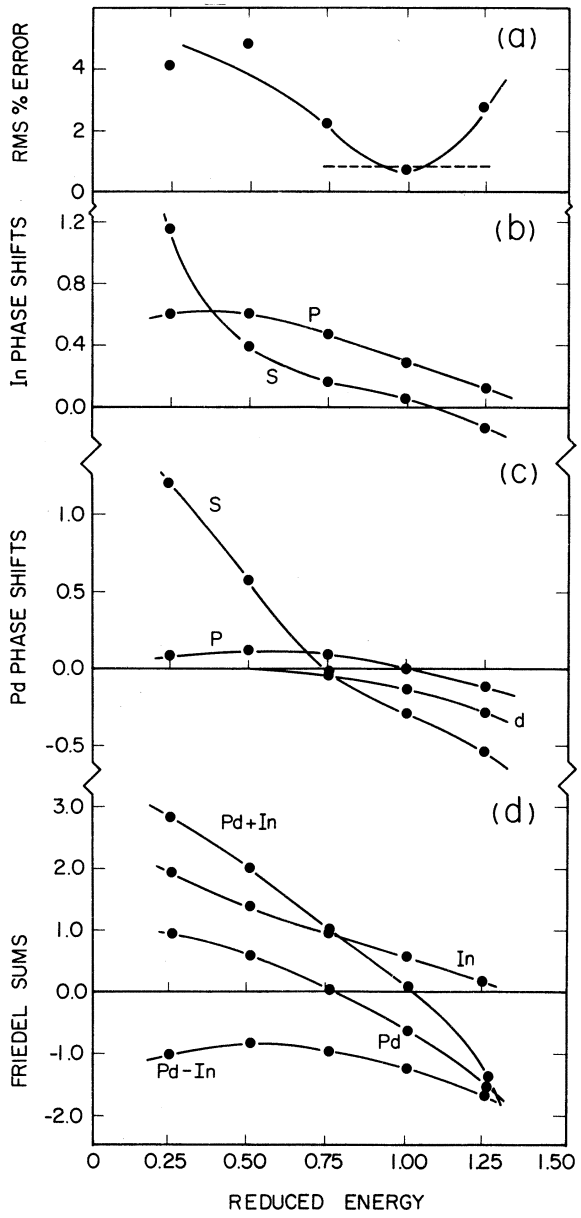

FIG. 5. (a) The rms fitting error as a function of energy/free-electron energy. The dashed line represents an estimate of experimental accuracy. (b) Fitted In phase shifts for s and p waves. (c) Fitted Pd phase shifts for s, p, and d waves. (d) Friedel sums for each atom: the sum and difference of the two atoms.

in free-electron energy units. The rms fitting error in Fig. 5(a) has a definite minimum near the free-electron value in contrast to the rather flat minima found in monatomic metals such as Sn,[14] alkali,[15] and noble[16–18] metals. This follows from the argument of Lee and Heine[16] who show that setting the energy parameter to the free-electron value is equivalent to choosing a "minimum-perturbation" potential. This potential causes the least breakdown of various approximations and assumptions used in the APW formalism. As the energy is shifted away from the free-electron value towards 0, the potential approaches the ionic potential. Setting the In d and other phase shifts with $l > 2$ zero becomes less valid for these stronger potentials. Unfortunately, the necessity of having five or six phase shifts even for a basic description of a diatomic system make it impossible to add further phase shift parameters when there are only six convenient data points. No check was made to see if the use of more parameters allowed better fits at energies away from the free-electron value. A similar argument based on the strength of Fourier potential coefficients is given by Devillers and de Vroomen.[14]

The fitted phase shifts as a function of energy are shown in Figs. 5(b) and 5(c) for In and Pd. All the phase shifts are smoothly varying functions of energy as expected. It is interesting to relate these phase shifts to Andersen's[19] crystal potential parameters shown in Table III. λ_l^2 is the energy at which the lth phase shift crosses zero. S_l is the radius at which the lth logarithmic derivative is energy independent. The S_l were determined from the "focusing points" of the logarithmic derivatives evaluated at $E = 0.75$, 1.0 and 1.25. Only the In p logarithmic derivative showed a slightly diffuse focus. According to Andersen, the S_l should all fall between the inscribed and exscribed spheres of the Wigner-Seitz cell, i.e., between 1.00 and 1.29 in units of Table III. There is a substantial deviation for two values. The free-electron value of λ_l is of course 1.00. The deviations found suggest a Fermi surface not far from a free-electron one as is found, in fact, the major differences being near R and M.

The Friedel sum truncated at $l = 2$ is

$$F = (2/\pi)(\epsilon_0 + 3\epsilon_1 + 5\epsilon_2) .$$

The F for the unit cell (both atoms) is shown in Fig. 5(d). This has the behavior expected for a system with 3 electrons/cell, being ~ 0 at the free-

TABLE III. Potential parameters[a] from the fits of PdIn phase shifts.

Material	l	S_l[b]	λ_l[c]
Pd	0	1.01 ± 0.08	0.86
	1	1.04 ± 0.01	1.00
	2	1.56 ± 0.02	0.7
In	0	0.71 ± 0.11	1.04
	1	1.04 ± 0.15	1.2

[a]Reference 19.

[b]S_l in units of inscribed radius. Then the exscribed radius is 1.29.

[c]λ_l in units of free-electron wave vector.

electron energy (E_0) and rising to ~ 3 at $\frac{1}{4}E_0$. Monatomic metals[14,16,18] have previously been found to follow this trend. A simple argument of Lee and Heine[16] suggests the curve goes as (Z is the valence)

$$F = Z - Z[E/E_0]^{3/2} . \quad (1)$$

A linear least-squares fit of F vs $(E/E_0)^{3/2}$ gives $F = 3.2-3.3(E/E_0)^{3/2}$. The Friedel sums for each atom are also shown in Fig. 5(d), where a least-squares fit gives for Pd $F = 1.2-1.8(E/E_0)^{3/2}$ and for In, $F = 2.0-1.5(E/E_0)^{3/2}$. An extension of Eq. (1) for each of these is

$$F_i = Z_i - \bar{Z}(E/E_0)^{3/2} ,$$

where $\bar{Z}$ is the average valence (1.5). The two slopes are in rough agreement with this. Note, however, that the apparent valences (the intercepts) are ~ 1 and ~ 2 for Pd and In rather 0 and 3 as expected from ionic considerations. This change suggests that charge transfer has taken place in the alloy. The plot of $F_{Pd}-F_{In}$ in Fig. 5(d) also shows a separation of ~ 1 electron. It is unclear whether the energy variation of this difference is significant or not. In any case approximately one electron has been transferred from the In to the Pd atom.

V. CONCLUSIONS

All three β brasses have essentially the same Fermi surface with each having only slight individual differences, in contrast to the remarks of Ref. 3. However, the range of sample quality makes the data only fair in AgZn, better in PdIn and best in CuZn. The strange disappearance of the octahedron orbit over large regions in CuZn probably was the main cause of interpretation difficulties. Skriver's calculations have shown that good agreement is obtained from first principles in AgZn and CuZn and the present paper describes how successful fits of data can be made with phase shifts as parameters in an APW formulation.

ACKNOWLEDGMENTS

I would like to thank Dr. J. -P. Jan for helpful discussions about the β brasses and for comments on the manuscript and Dr. P. T. Coleridge for conversations about the phase-shift methods. Useful suggestions have been provided by Dr. H. L. Skriver and Dr. P. M. Holtham.

---

*National Research Council of Canada Postdoctorate Fellow.

[1] J. -P. Jan, W. B. Pearson, and Y. Saito, Proc. R. Soc. A 297, 275 (1967).
[2] A. Karlsson, J. Low Temp. Phys. 1, 59 (1969).
[3] J. -P. Jan and C. M. Perrott, J. Low Temp. Phys. 8, 195 (1972).
[4] A. E. Dunsworth and J. -P. Jan, J. Low Temp. Phys. 13, 53 (1973).
[5] H. L. Skriver, Solid State Commun. 11, 1355 (1972).
[6] H. L. Skriver and N. E. Christensen, Phys. Rev. B 8, 3778 (1973).
[7] H. L. Skriver, Phys. Status Solidi 58, 721 (1973).
[8] A. E. Dunsworth (unpublished).
[9] S. J. Cho, Phys. Status Solidi 41, 179 (1970).
[10] H. L. Skriver (unpublished).
[11] J. -P. Jan (private communication).
[12] L. F. Mattheiss, J. H. Wood, and A. C. Switendick, *Methods in Computational Physics* (Academic, New York, 1968), Vol. 8, pp. 63–147.
[13] M. J. D. Powell, Comp. J. 7, 303 (1964).
[14] M. A. C. Devillers and A. R. de Vroomen, Solid State Commun. 9, 1939 (1971).
[15] M. J. G. Lee, Phys. Rev. 178, 953 (1969).
[16] M. J. G. Lee and V. Heine, Phys. Rev. B 5, 2829 (1972).
[17] M. J. G. Lee, Phys. Rev. 187, 901 (1969).
[18] J. C. Shaw, J. B. Ketterson, and L. R. Windmiller, Phys. Rev. B 5, 3894 (1972).
[19] O. K. Andersen, Phys. Rev. Lett. 27, 1211 (1971).